ORIGINAL ARTICLE

Chemerin has a protective role in hepatocellular carcinoma by inhibiting the expression of IL-6 and GM-CSF and MDSC accumulation

Y Lin[1,4], X Yang[1,4], W Liu[2,4], B Li[1], W Yin[1], Y Shi[2] and R He[1,3]

Hepatocellular carcinoma (HCC) is linked to inflammation and immunosuppression. Chemerin is highly expressed in the liver and implicated in the regulation of inflammation. However, the role of chemerin in HCC remains unclear. In this study, we aimed to investigate whether chemerin is able to influence HCC progression by regulating tumor-associated inflammation. Here we demonstrated that chemerin significantly decreased in blood and tumor tissues of HCC patients, and tumor chemerin levels were inversely associated with the prognosis. In an orthotopic mouse model of HCC, *Rarres2*$^{-/-}$ mice exhibited aggressive tumor growth and lung metastasis, whereas chemerin overexpression greatly inhibited tumor growth. The tumor-inhibitory effect of chemerin was accompanied by a shift in tumor-infiltrating immune cells from myeloid-derived suppressive cells (MDSCs) to interferon-γ$^+$T cells and decreased tumor angiogenesis. Furthermore, we demonstrated that the tumor-inhibitory effect of chemerin was partly dependent on T cells, as chemerin overexpression could inhibit tumor growth, albeit to a lesser extent, in *Rag1*$^{-/-}$ mice when compared with wild-type controls. Mechanistically, chemerin inhibited nuclear factor-κB activation and the expression of granulocyte-macrophage colony-stimulating factor (GM-CSF) and interleukin-2 (IL-6) by tumor cells and tumor-associated endothelial cell, respectively, via its receptors, and consequently, MDSC induction was impaired, leading to restoration of antitumor T-cell response and decreased tumor angiogenesis. Clinically, systemic and tumor levels of chemerin were found to inversely correlate with circulating concentrations of GM-CSF or IL-6 and tumor-infiltrating myeloid cells, respectively, in HCC patients. Moreover, neutralization of GM-CSF and IL-6 abrogated HCC progression and MDSC accumulation in *Rarres2*$^{-/-}$ mice. In conclusion, our study reveals the tumor-inhibitory effect of chemerin by suppressing inflammatory tumor microenvironment with therapeutic implications for inflammation-associated cancer-like HCC.

INTRODUCTION

Hepatocellular carcinoma (HCC) is a typical inflammation-associated cancer.[1] Hepatic inflammatory responses are considered to be the major contributor to HCC development by enhancing immunosuppression and angiogenesis, thereby providing permissive microenvironment for tumor cell growth and invasion.[1] HCC-associated inflammation is characterized by abundant expression of various pro-inflammatory cytokines within the tumor microenvironment, which in turn induces the generation, recruitment and activation of different immune cells including myeloid-derived suppressor cells (MDSCs). MDSCs are directly implicated in the promotion of tumor growth and metastasis by their potent immunosuppressive activities, particularly on T cells, and their abilities to promote angiogenesis.[2,3] MDSCs were recently reported to accumulate in the blood and tumor tissues of HCC patients,[4–6] and the frequency of circulating MDSC correlates with HCC recurrence.[5] Several inflammatory cytokines including interleukin-2 (IL-6), IL-1, granulocyte-macrophage colony-stimulating factor (GM-CSF), granulocyte

colony-stimulating factor, CXCL1/2 and CCL2 have been shown to be responsible for the induction and the migration of MDSCs.[7] Increased serum levels of these cytokines have been reported in HCC patients,[8] among which elevated IL-6 levels are associated with risk of HCC and poor prognosis.[9] Accumulating evidence implicates the critical role of GM-CSF and IL-6 in tumor development by inducing abundant MDSC accumulation. Tumor cell-derived GM-CSF has been demonstrated to promote tumor growth and metastasis by inducing the generation and systemic expansion of Gr-1$^+$CD11b$^+$ MDSCs.[10,11] IL-6 is also important for the expansion and the survival of MDSCs, which contributes to the development of several types of inflammation-associated cancer including HCC.[3,12]

Chemerin is widely distributed with particularly high levels in the liver of both human and mouse,[13,14] and is originally described as a chemoattractant for plasmacytoid dendritic cells and natural killer (NK) cells through its functional receptor CMKLR1.[13,15,16] CMKLR1 was recently reported to be expressed by non-leukocytes including epithelial cells and endothelial cells (ECs).[17,18] CCRL2 was

---

[1]Department of Immunology and Key Laboratory of Medical Molecular Virology of Ministries of Education and Health, School of Basic Medical Sciences, Shanghai, People's Republic of China; [2]Key Laboratory of Carcinogenesis and Cancer Invasion of Ministry of Education, Department of Liver Surgery, Liver Cancer Institute, Zhongshan Hospital, Shanghai, People's Republic of China and [3]Department of Immunology, Biotherapy Research Center, Fudan University, Shanghai, People's Republic of China. Correspondence: Associate Professor Y Shi, Key Laboratory of Carcinogenesis and Cancer Invasion of Ministry of Education, Department of Liver Surgery, Liver Cancer Institute, Zhongshan Hospital, 180 FengLin Road, Shanghai 200032, People's Republic of China or Professor R He, Department of Immunology, Shanghai Medical School, Fudan University, 138# Yixueyuan Road, Shanghai 200032, People's Republic of China.
E-mail: shi.yinghong@zs-hospital.sh.cn or ruihe@fudan.edu.cn
[4]These authors contributed equally to this work.

identified as atypical chemerin receptor with wide cellular distribution, functioning to present chemerin to CMKLR1.[19] Accumulating evidence from our studies and others suggest that chemerin–CMKLR1 axis could have either pro- or anti-inflammatory role depending on the context of tissue inflammation.[20,21] Recently, decreased chemerin was reported in several types of solid tumor, including HCC.[22–24] However, the role of chemerin in the development of inflammation-associated cancer such as HCC remain unclear.

In this study, we examined chemerin levels and its predictive role in HCC patients, and further investigated the role of chemerin in HCC growth/metastasis and tumor-associated inflammation by taking advantage of the newly established chemerin-deficient (*Rarres2*^{−/−}) mice and several mouse models of HCC.

RESULTS

HCC patients exhibit significantly decreased systemic and local expression of chemerin, and decreased tumor chemerin expression is associated with poor prognosis

The liver has been reported to be the most prominent source for chemerin in both human and mouse.[13,14] We found that HCC patients had much lower serum chemerin levels compared with healthy subjects (19.35 ± 3.333, fold reduction, $n = 24$, $P < 0.0001$; Supplementary Table S1 and Figure 1a). Furthermore, chemerin expression at mRNA and protein levels was significantly lower in tumor than para-tumor tissues from HCC patients (Figure 1b). In addition, several human HCC cell lines secreted significantly less chemerin than a normal liver cell line, LO2 cells (Figure 1c). These results show that chemerin is greatly down-regulated systemically and locally in HCC patients. To determine whether tumor chemerin levels correlated with the clinic outcome

of HCC patients, we next assessed chemerin expression in HCC tissue microarray (TMAs) by immunohistochemical (IHC) staining, and correlated tumor chemerin levels with relevant clinical information of HCC patients (Supplementary Table S2). We found that chemerin levels were positively associated with favorable clinical characteristics such as small tumor size, low-grade tumor differentiation and early Barcelona Clinic Liver Cancer stage (Supplementary Table S3). More importantly, HCC patients with higher chemerin levels had significantly higher survival rate of 1- and 3-year and significantly lower recurrence rate of 1- and 3-year than those with lower chemerin levels (Figure 1d). These data collectively indicate a potential protective role of chemerin in HCC.

Chemerin inhibits tumor growth and lung metastasis in mouse models of HCC

Prompted by the above clinical findings, we next investigated the role of chemerin in HCC progression by using several mouse models of HCC. First, we generated *Rarres2*^{−/−} mice (Supplementary Figures 1a–c) to investigate whether chemerin deficiency influenced an orthotopic HCC model by implanting tumor tissues derived from mouse HCC Hepa1-6 cells into the liver. *Rarres2*^{−/−} mice were viable and fertile and developed normally, and displayed normal numbers of myeloid and lymphoid cells in peripheral blood, spleens and liver under steady state (Supplementary Figure 1d). Furthermore, no obvious pathological changes were observed in major organs including liver, kidney, colon, lung, spleen of *Rarres2*^{−/−} mice compared with those of wild-type (WT) littermates (Supplementary Figure 1e). Hepa1-6 cells secreted very little, if any, chemerin, but express CMKLR1 and CCRL2 (Supplementary Figures 2a and b). *Rarres2*^{−/−} mice implanted with Hepa1-6 tumor exhibited significantly
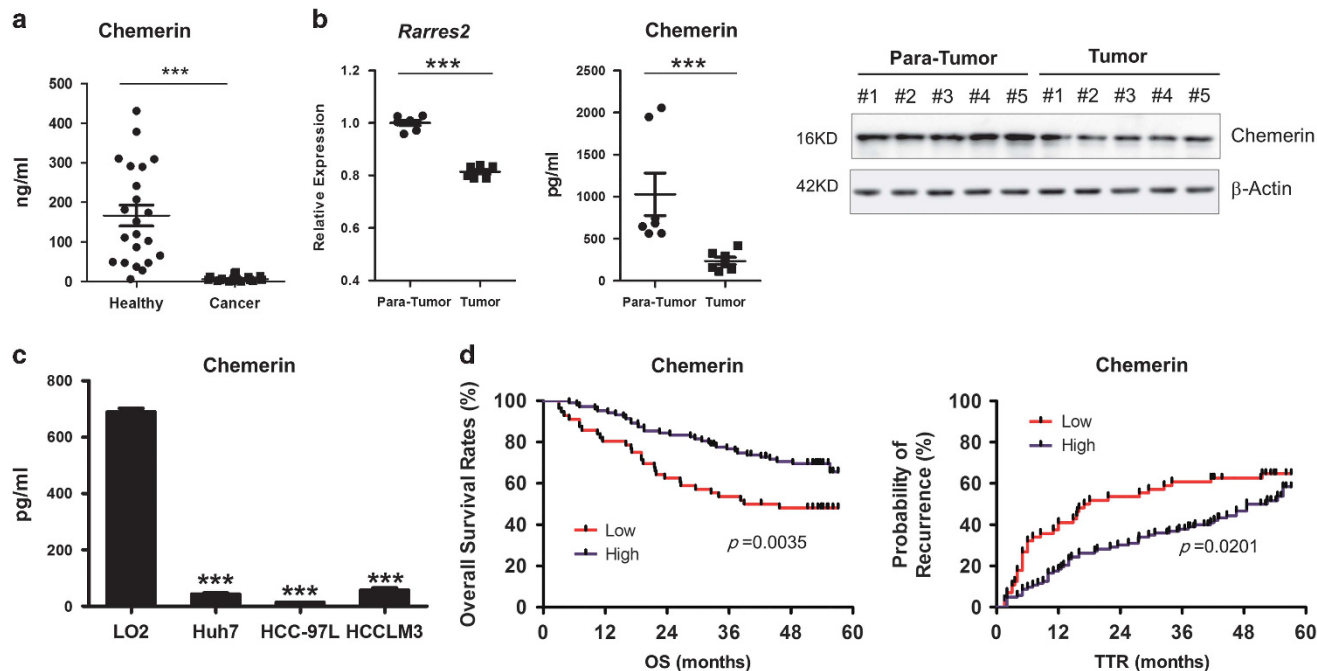

Figure 1. Chemerin levels are downregulated in blood and tumor tissues of HCC patients, which predicts the poor clinical outcomes. (**a**) Chemerin protein levels were measured by enzyme-linked immunosorbent assay (ELISA) in sera from healthy subjects and HCC patients ($n = 24$). (**b**) Freshly resected tumor and para-tumor tissues from surgical specimens of HCC patients were collected. Left: gene expression of chemerin was determined by quantitative reverse transcriptase (qRT)–PCR; middle and right: protein levels of chemerin were measured by ELISA and western blot. ***$P < 0.001$. (**c**) Chemerin concentrations were measured by ELISA in the culture of a normal liver cell line LO2 and several human HCC cell lines including Huh7, HCC-97L and HCCLM3. Values are mean ± s.e.m. of three replicate wells from a representative of three experiments. ***$P < 0.001$ vs LO2. (**d**) Kaplan–Meier survival or recurrence analysis of human HCC TMA based on chemerin density following IHC staining. Chemerin density was coded as low or high, using the median value as a cutoff point. $n = 156$. OS, overall survival; TTR, time to recurrence.
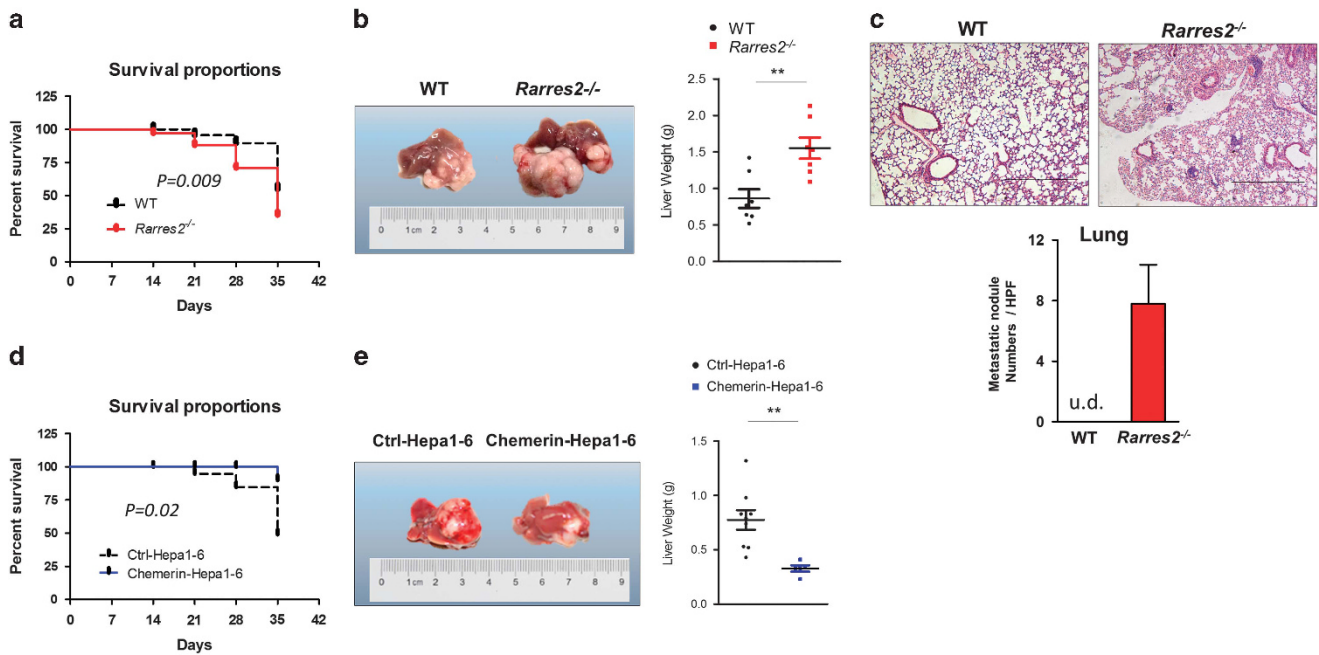
Figure 2. Chemerin inhibits tumor progression in mouse models of HCC. (**a**) Kaplan–Meier plot of survival of WT and Rarres2$^{-/-}$ mice implanted with Hepa1-6 cells in an orthotopic HCC model. $n = 16$–18. (**b**) Representative images of liver tumors and the liver weight. (**c**) Left, representative images of hematoxylin and eosin (H&E)-stained lung sections. Right, numbers of metastatic nodules counted in a 100X high-power field (HPF). Original magnification, ×100; scale bar, 100 μm. (**d**) Kaplan–Meier plot of survival of WT mice implanted with Ctrl-Hepa1-6 cells or chemerin-overexpressing Hepa1-6 cells in an orthotopic HCC model. $n = 12$–14. (**e**) Representative images of liver tumors and the liver weight. Columns and error bars represent mean ± s.e.m. ($n = 12$–18 per group). **$P < 0.01$, ***$P < 0.001$. Similar results were obtained from three independent experiments.

increased mortality rate compared with similarly treated WT littermates (Figure 2a). All the mice were killed on day 35 because only about 30% Rarres2$^{-/-}$ mice survived. Rarres2$^{-/-}$ mice had much larger liver tumors and higher liver weight than WT littermates (Figure 2b). As expected, no metastatic tumor nodules were found in hematoxylin and eosin-stained lung sections from WT littermates, as Hepa1-6 is a low metastatic cell line (Figure 2c). Intriguingly, apparent tumor nodules were found in lung sections of Rarres2$^{-/-}$ mice (Figure 2c). To further confirm the HCC-inhibitory effect of chemerin, we forced chemerin expression in Hepa1-6 cells (chemerin-Hepa1-6) (Supplementary Figure 2a), and vector-transfected Hepa1-6 cells were used as control (Ctrl-Hepa1-6). In contrast to aggravated tumor growth in Rarres2$^{-/-}$ mice, chemerin overexpression significantly decreased mortality rate, liver tumor growth and liver weight of WT mice implanted with Hepa1-6 tumors (Figures 2d and e). We also confirmed the tumor-inhibitory effect of chemerin in a subcutaneous tumor model of HCC (Supplementary Figure 2c). Furthermore, Rarres2$^{-/-}$ mice had significantly more metastatic nodules than WT littermates by using a lung metastasis model by intravenously injecting Hepa1-6 cells (Supplementary Figure 3a). In contrast, WT mice intravenously injected with chemerin-Hepa1-6 cells had significantly less metastatic nodules than those with Ctrl-Hepa1-6 cells (Supplementary Figure 3b). Collectively, these data demonstrate that chemerin inhibits HCC growth and lung metastasis.

Chemerin suppresses tumor-promoting microenvironment by shifting the infiltrating immune cells from MDSCs to IFN-γ$^+$ T cells
We excluded the possibility that HCC-inhibitory effect of chemerin was due to its ability to directly inhibit Hepa1-6 cell growth, as chemerin overexpression or addition of exogenous chemerin had no effect on the proliferation and apoptosis of Hepa1-6 cells in vitro (Supplementary Figures 4a–c and data not shown). We

therefore speculated that chemerin could modulate the tumor microenvironment to inhibit HCC progression. We first analyzed immune cell composition in Hepa1-6 tumor tissues from WT and Rarres2$^{-/-}$ mice by flow cytometry. Significantly increased proportions of Gr-1$^+$CD11b$^+$ MDSCs and F4/80$^+$CD11b$^+$ tumor-associated macrophages (TAMs) were found in Hepa1-6 tumors from Rarres2$^{-/-}$ mice compared with those from WT littermates (Figure 3a). These findings were further supported by IHC staining showing significant more Gr-1-positive or F4/80-positive cells observed in tumor sections from Rarres2$^{-/-}$ mice (Figure 3b). Consistently, the expression of genes that are closely related to MDSCs and TAM also significantly increased in tumors from Rarres2$^{-/-}$ mice (Figure 3c). In contrast, significantly decreased tumor-infiltrating CD4$^+$ and CD8$^+$ T cells that expressed interferon (IFN)-γ were found in Rarres2$^{-/-}$ mice compared with WT littermates (Figure 3d). This could be due to impaired T-cell proliferation, as significantly decreased percentages of CD4$^+$Ki67$^+$ and CD8$^+$ Ki67$^+$ were found in tumors from Rarres2$^{-/-}$ mice (Figure 3d). Conversely, chemerin overexpression caused a significant shift from infiltrating MDSCs to IFN-γ$^+$ T cells in orthotopic Hepa1-6 tumors (Supplementary Figures 5a and b). MDSCs mainly consist of two subsets, PMN-MDSCs and M-MDSCs, based on the expression level of Gr-1.[25] We found that chemerin significantly reduced infiltrating Gr1^{Hi}CD11b$^+$PMN-MDSCs, but only slightly reduced Gr-1^{mid}CD11b$^+$M-MDSCs (Supplementary Figures 6a and b). We further confirmed the immunosuppressive ability of each subset by showing that co-culture of Gr1^{Hi}CD11b$^+$PMN-MDSCs or Gr1^{mid}CD11b$^+$M-MDSCs significantly inhibited CD3$^+$T-cell proliferation upon anti-CD3/28 stimulation (Supplementary Figure 6c). There was no difference in tumor-infiltrating Tregs and plasmacytoid dendritic cells regardless of chemerin expression (data not shown). Although previous study showed that chemerin overexpression induces more infiltrating NK cells, which mediates its tumor-inhibitory effect in mouse model of melanoma,[24] similar percentages
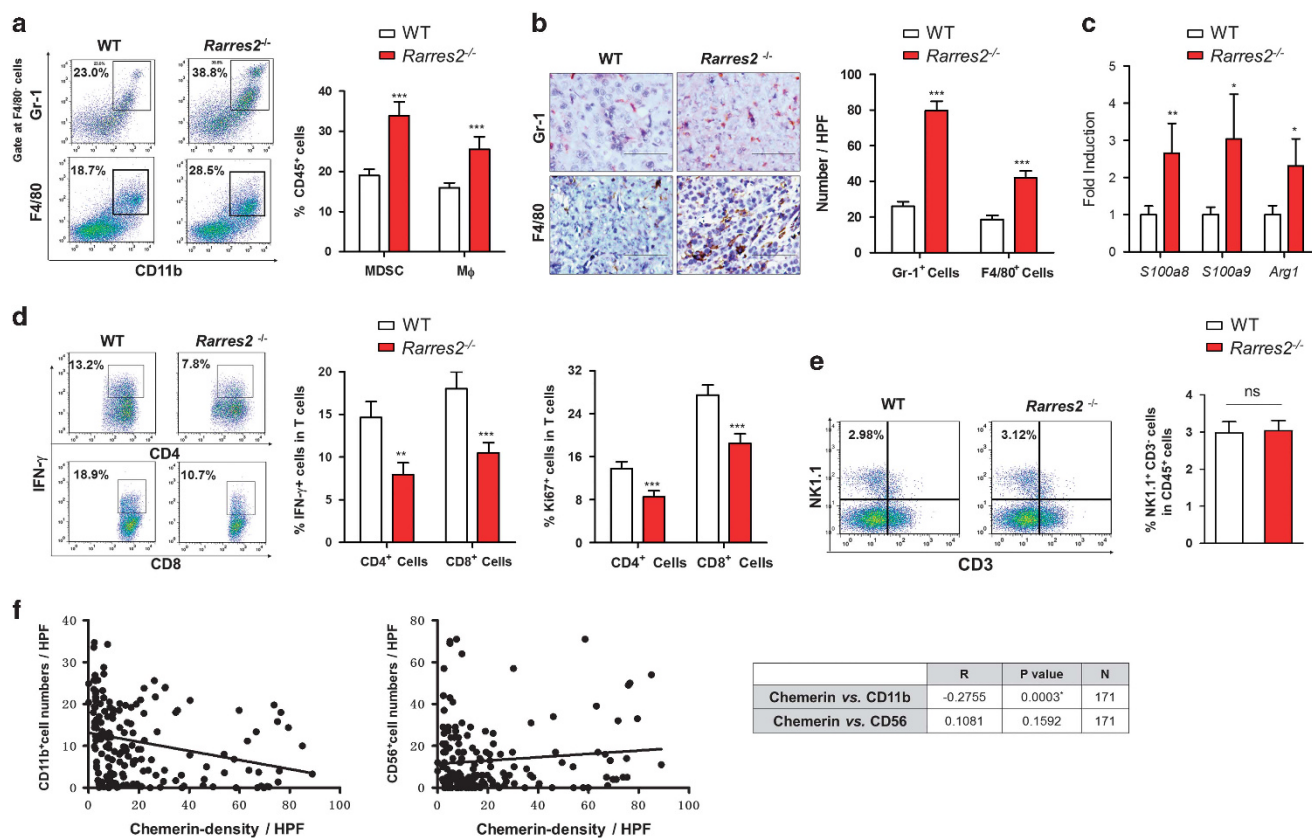
Figure 3. *Rarres2*$^{-/-}$ mice exhibit increased MDSC infiltration and decreased antitumor T-cell infiltration in orthotopic HCC tumors. (**a**) Representative flow cytometry data and averaged percentages of MDSCs and macrophages in enzymatically dissociated Hepa1-6 tumor tissues. Gr-1$^+$CD11b$^+$cells gated at F4/80-negative cells were considered as MDSCs and F4/80$^+$CD11b$^+$ cells as macrophages. (**b**) Left, representative images of IHC staining of Gr-1 and F4/80 in sections from Hepa1-6 tumors of WT or *Rarres2*$^{-/-}$ mice. Original magnification, ×400; scale bar, 50 μm. Right, numbers of Gr-1$^+$ and F4/80$^+$ cells were counted in a 200X high-power field (HPF). (**c**) Quantitative reverse transcriptase (qRT)–PCR analysis of the expression of genes that are related to MDSCs and macrophages in tumor tissues from WT or *Rarres2*$^{-/-}$ mice. (**d**, **e**) Representative flow cytometry data and averaged percentages of IFN-γ$^+$CD8$^+$ T cells and IFN-γ$^+$CD4$^+$ T cells, as well as Ki67$^+$CD4$^+$ T cells and Ki67$^+$CD8$^+$ T cells (**d**) and representative flow cytometry data and averaged percentages of NK cells (NK1.1$^+$CD3$^-$) (**e**) in enzymatically dissociated Hepa1-6 tumor tissues from WT or *Rarres2*$^{-/-}$ mice. (**f**) Chemerin density from each sample of human HCC TMA was plotted against numbers of CD11b$^+$ myeloid cells or CD56$^+$ NK cells in tumors from the same patient. A Pearson correlation was used to evaluate the association of chemerin density and the numbers of CD11b$^+$ or CD56$^+$ cells. $n = 171$. Columns and error bars represent mean ± s.e.m. ($n = 5$–8 per group). *$P < 0.05$, **$P < 0.01$, ***$P < 0.001$. Similar results were obtained from three independent experiments.

of tumor-infiltrating NK cells were found in Hepa1-6 tumors of *Rarres2*$^{-/-}$mice or chemerin- Hepa1-6 tumors when compared with respective controls (Figure 3e and Supplementary Figure 5c). Our results collectively suggest that chemerin inhibits tumor infiltration of MDSCs and TAMs, which may in turn lead to enhanced antitumor T-cell responses.

We next sought clinic evidence of the link between chemerin and infiltrating myeloid cells in HCC. Given the majority of CD11b$^+$ cells consisting of MDSCs and TAMs, we analyzed the correlation between CD11b-expressing cells and chemerin levels by performing IHC staining of HCC TMAs. We found that tumor chemerin levels inversely correlated with the numbers of infiltrating CD11b-expressing cells (Figure 3f). Moreover, we confirmed that chemerin had no effect on tumor infiltration of NK cells in human HCC samples, as there was no correlation between chemerin levels and CD56-expressing NK cells (Figure 3f).

The tumor-inhibitory effect of chemerin is partly reserved in *Rag1*$^{-/-}$ mice

As we found that chemein influenced tumor-infiltrating IFN-γ$^+$ T cells, but not NK cells, we next investigated whether T cells were required by the HCC-inhibitory effect of chemerin. Chemerin

overexpression inhibited tumor growth and volumes in *Rag1*$^{-/-}$ mice in a significantly lesser extent than that in WT mice (Figure 4a), indicating the involvement of T-cell immunity in the tumor-inhibitory effect of chemerin. Considering that CD4$^+$T cells consist of different subsets with either tumor-inhibiting or tumor-promoting ability and CD8$^+$T cells are the primary antitumor effector T cells, we chose to deplete CD8$^+$T cells to further differentiate the roles of CD4$^+$ and CD8$^+$T cells in the tumor-inhibitory effect of chemerin. Similarly, depletion of CD8$^+$T cells partly impaired the HCC-inhibitory effect of chemerin in similar level to those observed in *Rag1*$^{-/-}$ mice (Figure 4b). These results show that the tumor-inhibitory effect of chemerin is partly dependent on T cells, especially CD8$^+$T cells. Notably, chemerin-Hepa1-6 tumors grew much slower and smaller than Ctrl-Hepa1-6 tumors in *Rag1*$^{-/-}$ mice or CD8$^+$T-cell-depleted mice (Figures 4a and b), indicating the involvement of other T-cell independent tumor-inhibitory mechanism. As expected, chemerin overexpression significantly reduced tumor-infiltrating MDSCs and TAM in *Rag1*$^{-/-}$ mice (Figure 4c). In addition to their immunosuppressive activity, MDSCs and TAMs also contribute to tumor growth by promoting tumor angiogenesis.[26] Consistently, greatly decreased angiogenesis was observed in chemerin-Hepa1-6 tumors of *Rag1*$^{-/-}$ mice, as evidenced by much
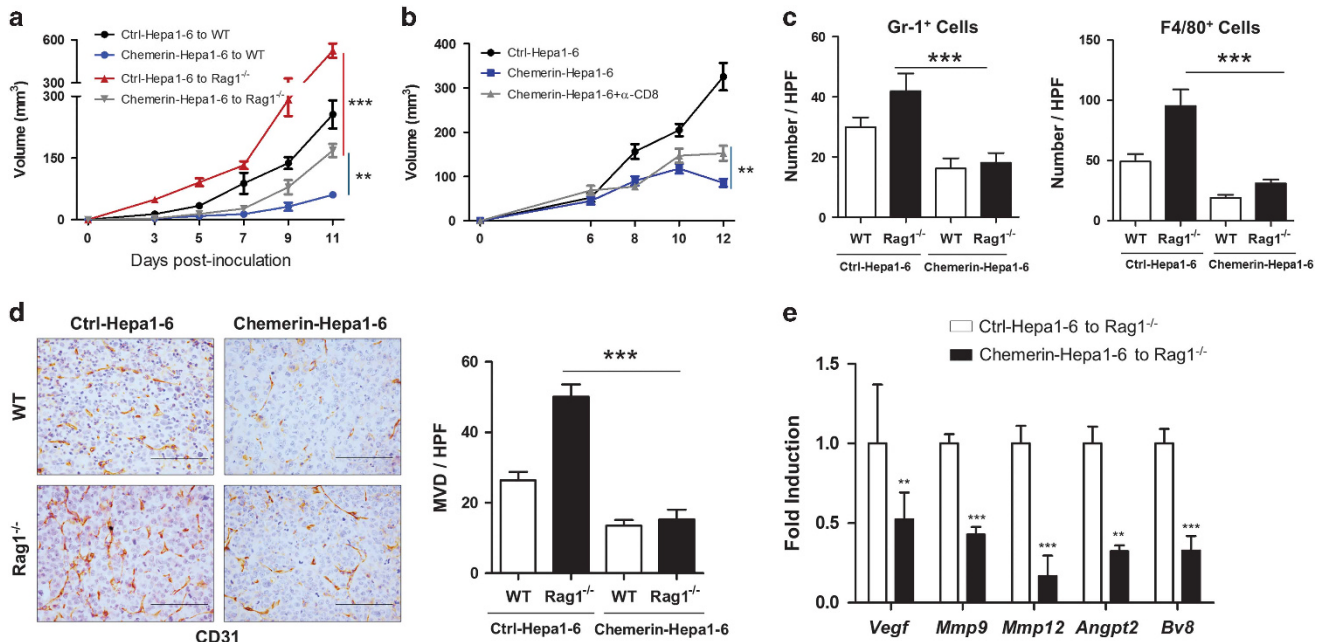
Figure 4. The tumor-inhibitory effect of chemerin is partly reserved in *Rag1*$^{-/-}$ mice. (**a**, **b**) Ctrl-Hepa1-6 and chemerin-Hepa1-6 cells were injected subcutaneously into male C57BL/6 WT and *Rag1*$^{-/-}$ mice (**a**), and some WT mice were randomized to be intraperitoneally injected with anti-CD8 neutralizing antibody (200 μg/mouse) every 3 days from 3 days before inoculation of tumor cells until mice were killed (**b**). Tumor growth was measured at the indicated time points. (**c**) Numbers of Gr-1$^+$ and F4/80$^+$ cells counted in tumor sections following IHC staining. (**d**) Left, representative photomicrographs of IHC staining of CD31 in tumor sections. Right, microvessel density (MVD) was calculated by surface quantification of CD31-positive cells. Statistical significance calculated by analysis of variance (ANOVA). Original magnification, × 200; scale bar, 50 μm. (**e**) Quantitative reverse transcriptase (qRT)–PCR analysis of the expression of proangiogenic genes in tumor tissues from *Rag1*$^{-/-}$ mice that received Ctrl-Hepa1-6 and chemerin-Hepa1-6 cells. Columns and error bars represent mean ± s.e.m. (*n* = 6 per group). *$P < 0.05$, **$P < 0.01$, ***$P < 0.001$. Similar results were obtained from two independent experiments.

less CD31$^+$ cells and significantly decreased expression of various angiogenic factors when compared with Ctrl-Hepa1-6 tumors (Figures 4d and e). These data collectively demonstrate that the HCC-inhibitory effect of chemerin could be attributed to decreased tumor-infiltrating MDSCs, leading to restored T-cell immunity and reduced angiogenesis.

Chemerin reduces systemic MDSC induction and the expression of GM-CSF and IL-6 in HCC-bearing mice

We next explored the mechanism underlying the inhibitory effect of chemerin on MDSC accumulation. To determine whether decreased tumor-infiltrating MDSCs was due to the impairment in MDSC induction or migration, we examined the influence of chemerin on systemic MDSC accumulation in the blood and the spleens of HCC-bearing mice. *Rarres2*$^{-/-}$ mice had significantly increased MDSC accumulation in both circulation and spleens, whereas chemerin overexpression significantly reduced systemic MDSC accumulation (Figure 5a). Similar results were obtained in lung metastatic model (Supplementary Figures 7a and b). We next examined the gene expression of a variety of soluble factors, which have been reported to participate in the generation, migration and activities of MDSCs, in tumor tissues. We found that GM-CSF, IL-6 and IL-4 were mostly affected by chemerin in Hepa1-6 tumors, as lack of chemerin significantly increased, whereas chemerin overexpression significantly decreased, their gene expression. However, chemerin had no effect on the expression of chemokines that are important for tumor recruitment of MDSC, such as CCL2 and CXCL1/2 (Figure 5b). Consistently, chemerin overexpression did not affect the MDSC chemotactic activity of Hepa1-6 cell supernatants (Supplementary Figure 8a).

Although serum levels of both GM-CSF and IL-6 were undetectable in mice of all groups, Compared with healthy controls, HCC patients had significantly increased serum levels of GM-CSF (5.92 ± 0.48 vs 4.87 ± 0.32 pg/ml, *n* = 24, $P < 0.05$) and IL-6 (72.36 ± 18.5 vs 4.09 ± 2.18 pg/ml, *n* = 24, $P < 0.001$). Moreover, serum levels of chemerin conversely correlated with those of GM-CSF and IL-6 in individual HCC patient, albeit only the association between chemerin and IL-6 reaching significance (Figure 5c). Considering greatly impaired systemic accumulation of MDSCs in *Rarres2*$^{-/-}$ mice and the importance of GM-CSF and IL-6 for MDSC induction, these data together suggest that chemerin could indirectly interfere with MDSC induction by inhibiting GM-CSF and IL-6 expression, consequently leading to reduced tumor infiltration of MDSCs.

Chemerin targets tumor cells and tumor-associated ECs to inhibit the expression of GM-CSF and IL-6 and NF-κB activation, which is mediated by its receptors

To analyze cell-type-specific expression of each cytokine and determine the target cells of chemerin, we purified various cell populations from fresh Hepa1-6 tumors based on the expression of cell-type-specific marker (Figure 6a), and assessed gene expression of GM-CSF and IL-6 in individual populations. We demonstrated that tumor cells themselves were the major cell source for GM-CSF and tumor-associated ECs for IL-6 (Figure 6a). Moreover, tumor cells and ECs derived from Hepa1-6 tumors of *Rarres2*$^{-/-}$ mice expressed much higher levels of GM-CSF and IL-6, respectively, whereas those from chemerin-Hepa1-6 tumors of WT mice expressed much lower levels of two cytokines, respectively, when compared with the respective controls (Figure 6b). Both GM-CSF and IL-6 are target genes of nuclear factor (NF)-κB that has been implicated in the initiation and the
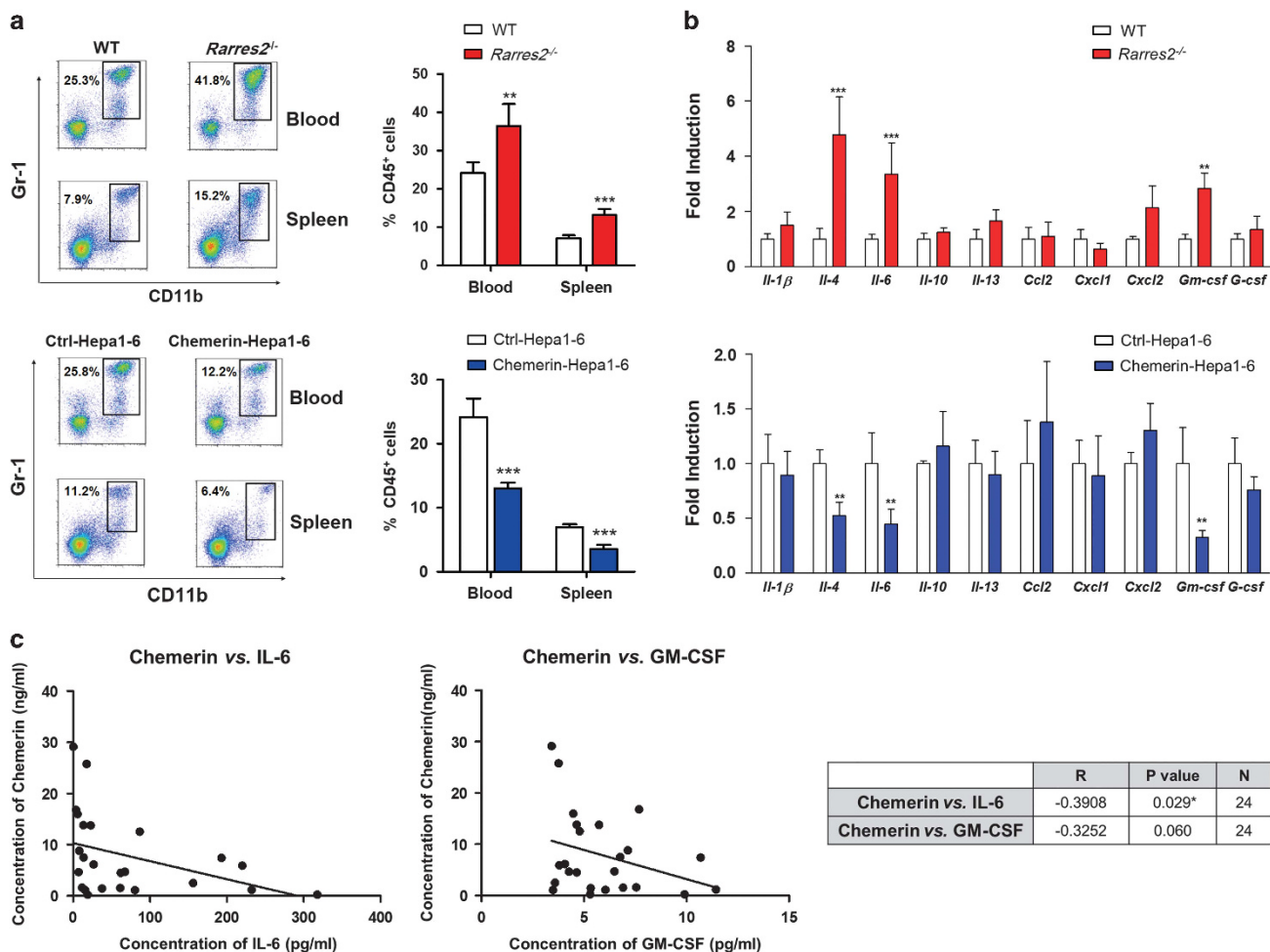
Figure 5. Chemerin inhibits systemic MDSC accumulation and the expression of GM-CSF and IL-6 in HCC-bearing mice. (**a**) Representative flow cytometry data and averaged percentages of MDSCs in blood and spleen of HCC-bearing WT or Rarres2$^{-/-}$ mice (upper) and WT mice implanted with Ctrl-Hepa1-6 cells or chemerin-Hepa1-6 cells (lower) in orthotopic HCC model. (**b**) Quantitative reverse transcriptase (qRT)–PCR analysis of the expression of inflammatory genes that are responsible for MDSC biology in orthotopic HCC tissues from WT or Rarres2$^{-/-}$ mice (upper) and WT mice implanted with Ctrl-Hepa1-6 cells or chemerin-Hepa1-6 cells (lower). (**c**) The serum concentration of chemerin in each HCC patient was plotted against concentrations of IL-6 or GM-CSF in serum from the same patient. A Pearson correlation was used to evaluate the association of chemerin and of IL-6 or GM-CSF. Columns and error bars represent mean ± s.e.m. (n = 5–8 per group). *P < 0.05, **P < 0.01, ***P < 0.001. Similar results were obtained from three independent experiments in **a** and **b**.

promotion of HCC.[27,28] We found that tumor cells and ECs isolated from Hepa1-6 tumors of Rarres2$^{-/-}$ mice had higher levels of p-p65 than those from WT littermates, whereas chemerin overexpression caused lower p-p65 levels in tumor cells and ECs (Figure 6c), suggesting that chemerin was able to inhibit NF-κB activation.

We further examined the expression of CMKLR1 and CCRL2 on individual populations derived from Hepa1-6 tumors. Both were detected in tumor cells and tumor-associated ECs at higher levels, and MDSCs at lower levels, but undetectable in tumor-associated fibroblasts (Figure 6d). The interaction between chemerin–CMKLR1 or CCRL2 was confirmed by pulldown assay (Supplementary Figure 8). The direct effect of chemerin on the proliferation and migration of MDSCs was excluded (Supplementary Figures 9b and c). These data suggested tumor cells and tumor-associated ECs as target cells for chemerin in HCC microenvironment. This was further supported by in vitro studies. Chemerin overexpression significantly reduced GM-CSF secretion by Hepa1-6 cells, with no effect on CMKLR1 expression (Figure 6e and Supplementary Figure 2b). To mimic tumor-associated ECs, we stimulated bEND.3 cells, a mouse EC line

that expressed both CMKLR1 and CCRL2,[17] with Hepa1-6 cell supernatants. Very little IL-6 was secreted by bEND.3 cells, and supernatants from Ctrl-Hepa1-6 cells induced much more IL-6 secretion than those from chemerin-Hepa1-6 cells (Figure 6f). To test whether the inhibitory effect of chemerin on cytokine production was dependent on its receptors, we downregulated the expression of Cmklr1 or Ccrl2 in Hepa1-6 and bEND.3 cells by small interfering RNA. Knockdown of Cmklr1 or Ccrl2 completely restored the levels of GM-CSF and IL-6 in the cultures of chemerin-Hepa1-6 cells and bEND.3 cells stimulated with chemerin-Hepa1-6 cell supernatants, respectively (Figures 6e and f). We also confirmed the inhibitory effect of chemerin on NF-κB activation was dependent on its receptors (Figures 6e and f). GPR1 was reported to be the third receptor of chemerin, although its functional relevance is largely unknown.[20,29] However, specific knockdown of GPR1 did not affect GM-CSF secretion by Hepa1-6 cells and IL-6 by ECs (data not shown), indicating a dispensable role of GPR1. Collectively, these data demonstrate that chemerin has an anti-inflammatory role by targeting tumor cells and tumor-associated ECs to inhibit NF-κB activation and expression of GM-CSF and IL-6 in HCC microenvironment.
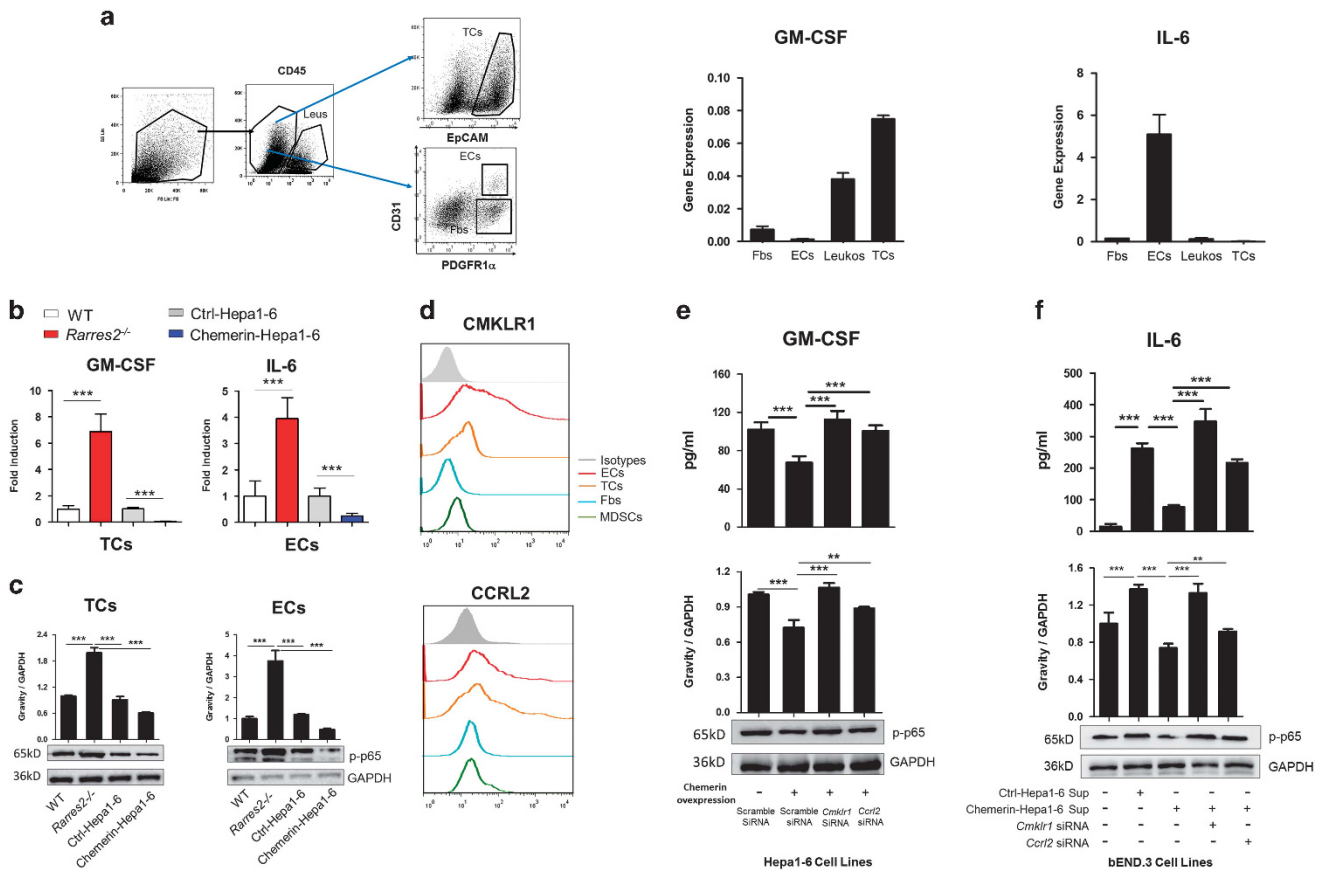
Figure 6. Chemerin inhibits the production of GM-CSF and IL-6 and NF-κB activation in tumor cells and tumor-associated ECs, respectively, which is mediated by its receptors. (**a**) Left, the gating strategy and the lineage marker used for isolation of individual cell populations from Hepa1-6 tumor tissue. Epithelial tumor cells (EpCAM$^+$), leukocytes (CD45$^+$), ECs (CD31$^+$PGDFR1α^+) and fibroblasts (Fb) (CD31$^-$PGDFR1α^+). Right, quantitative reverse transcriptase (qRT)–PCR analysis of gene expression of GM-CSF and IL-6 in individual cell populations sorted from Hepa1-6 tumor tissues. To quantitate the absolute gene expression of GM-CSF or IL-6 by individual cell populations in tumors, the values of $2^{\Delta}C_{(t)}$ of each gene multiply the percentage of individual cell populations in tumors. $n = 3$. (**b**, **c**) qRT–PCR analysis of gene expression of GM-CSF and IL-6 (**b**) and representative western blots showing phosphorylated p65 (p-p65) (**c**) in tumor cells and tumor-associated ECs, respectively. Tumor cells and tumor-associated ECs were isolated from Hepa1-6 tumors of WT and $Rarres2^{-/-}$ mice, as well as from Ctrl-Hepa1-6 tumors and chemerin- Hepa1-6 tumors of WT mice. $n = 3$. (**d**) Representative flow cytometry data of the expression of CMKLR1 and CCRL2 in individual cell populations sorted from Hepa1-6 tumor tissues in WT mice. (**e**) GM-CSF concentrations (upper) and p-p65 levels (lower) in Ctri-Hepa1-6 cells and chemerin-overexpressing Hepa1-6 cells, which were transfected with scramble small interfering RNA (siRNA) or $Cmklr1$ siRNA or $Ccrl2$ siRNA. (**f**) IL-6 concentrations (upper) and p-p65 levels (lower) in bEND.3 EC cells. bEND.3 cells were stimulated with or without supernatants from Ctrl-Hepa1-6 cells or chemerin-overexpressing Hepa1-6 cells, which were transfected with scramble siRNA or $Cmklr1$ siRNA or $Ccrl2$ siRNA. Columns and error bars represent of three replicate wells from a representative of three independent experiments. ***$P < 0.001$.

Neutralization of GM-CSF and IL-6 reverses aggravated orthotopic HCC progression and MDSC accumulation in $Rarres2^{-/-}$ mice

To further investigate whether GM-CSF and IL-6 mediate inhibitory effects of chemerin on HCC growth and MDSC accumulation *in vivo*, we neutralized GM-CSF and IL-6 in $Rarres2^{-/-}$ mice following orthotopically implanted Hepa1-6 tumors. Neutralization of GM-CSF and IL-6 markedly improved the survival of tumor-bearing $Rarres2^{-/-}$ mice and significantly reduced the increases in Heap1-6 tumor volumes and liver weight, as well as lung metastatic nodules (Figures 7a and b). Consistently, neutralization of GM-CSF and IL-6 significantly reduced tumor-infiltrating MDSCs and TAMs and systemic MDSC accumulation, enhanced tumor-infiltrating IFN-γ$^+$ T cells and reduced tumor angiogenesis in Hepa1-6 tumors of $Rarres2^{-/-}$ mice (Figures 7c-e). In addition, we also demonstrated that the administration of murine GM-CSF and IL-6 recombinant proteins abrogated the inhibitory effects of chemerin on tumor growth and MDSC accumulation, which was accompanied by reduced antitumor T-cell response and increased

tumor angiogenesis in a subcutaneous model of HCC (Supplementary Figures 10a-f). These data collectively demonstrate that HCC-inhibitory effect of chemerin is dependent on its ability to inhibit the production of GM-CSF and IL-6.

DISCUSSION

We here identify chemerin as a negative regulator of HCC-associated inflammation and immunosuppression, which provides protection against HCC development. Mechanistically, chemerin could inhibit NF-κB activation and the production of GM-CSF and IL-6 by directly acting on tumor cells and tumor-associated ECs, respectively, which leads to impaired MDSC accumulation, thereby providing a better tumor-suppressing microenvironment characterized by restored antitumor T-cell immunity and reduced tumor angiogenesis (Figure 7f).

We reported that systemic and local chemerin protein levels are downregulated in HCC patients, and decreased tumor chemerin levels are associated with the poor clinic outcome. Moreover, we
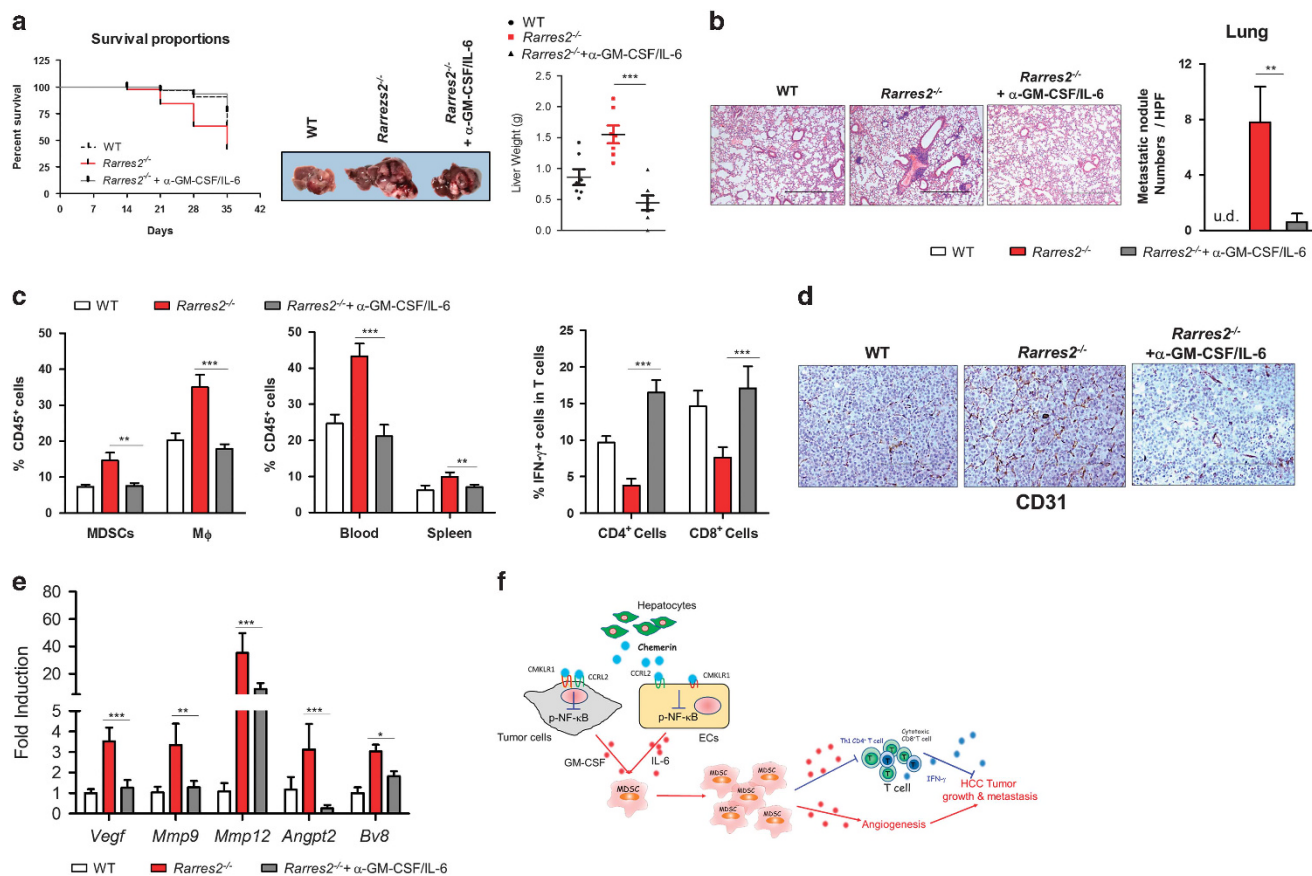
Figure 7. Neutralization of GM-CSF and IL-6 reverses aggravated orthotopic HCC progression and MDSC accumulation in *Rarres2*$^{-/-}$ mice. (**a**) Kaplan–Meier plot of survival and representative images of liver tumors and the liver weight. of WT mice and *Rarres2*$^{-/-}$ mice received isotype antibodies or neutralizing antibodies for GM-CSF and IL-6 in an orthotopic HCC model. $n = 16$. (**b**) Representative images of hematoxylin and eosin (H&E)-stained lung sections and numbers of metastatic nodules counted in a 100X high-power field (HPF). (**c**) The percentages of MDSCs and macrophages in tumor tissues and MDSCs in blood and spleens, as well as IFN-γ$^+$CD8$^+$ T cells and IFN-γ$^+$ CD4$^+$ T cells in tumor tissues. (**d**) Representative images of IHC staining of CD31. (**e**) Quantitative reverse transcriptase (qRT)–PCR analysis of the expression of proangiogneic genes in tumor tissues. Original magnification, × 200; scale bar, 50 μm in **b** and **d**. Columns and error bars represent mean ± s.e.m. ($n = 7$ per group). Similar results were obtained from two independent experiments. **$P < 0.01$, ***$P < 0.001$. (**f**) Schematic diagram of the cellular and molecular mechanism by which chemerin suppresses HCC progression.

demonstrated that chemerin has a protective role in HCC growth, as *Rarres2*$^{-/-}$ mice exhibited exaggerated orthotopic HCC growth, whereas chemerin overexpression inhibited tumor growth. Notably, chemerin deficiency caused lung metastasis of orthotopic HCC, highlighting a critical role of chemerin in restraining HCC tumor progression. We further revealed that HCC-inhibitory effect of chemerin is mediated by its ability to suppress tumor-promoting inflammation. First, chemerin did not affect the survival and proliferation of Hepa1-6 cells. Second, *Rarres2*$^{-/-}$ mice had exaggerated tumor-associated inflammation characterized by increased expression of GM-CSF and IL-6, and tumor accumulation of MDSCs and TAMs, moreover, neutralization of both cytokines almost reversed aggravated tumor progression in *Rarres2*$^{-/-}$ mice. Third, the serum chemerin levels was inversely associated with those of GM-CSF and IL-6 in HCC patients, indicating a negative regulatory role of chemerin in these two cytokines.

We further identified tumor cells and tumor-associated ECs as target cells of chemerin in the tumor microenvironment. Although B16 melanoma cells were reported to lack chemerin receptors,[24] we found Hepa1-6 cells expressed both receptors of chemerin. Whether tumor cells express chemerin receptors could be dependent on the tumor origin, as normal hepatocytes, but not melanocytes, were reported to express CMKLR1.[30]

Interestingly, chemerin acted on Hepa1-6 cells to selectively inhibit GM-CSF production with no effect on their proliferation and survival. Although previous studies suggested that IL-6 is secreted by tumor cells and infiltrating myeloid cells,[31] we unexpectedly found that tumor-associated ECs are the major cell source of IL-6 in our HCC models. This is supported by a recent study showing that ECs orchestrate the production of cytokines including IL-6 and infiltration of immune cells such as neutrophils in influenza virus-infected mice.[32] Thus, our study pointed out that EC, in addition to its well-known role in tumor angiogenesis, could serve as an active factor in tumor-associated inflammation by secreting IL-6. Furthermore, we demonstrated that disruption of chemerin or its receptors reduced IL-6 production by tumor-associated ECs, which is also consistent with a recent study showing that the act of chemerin–CMKLR1 on non-leukocytes, most likely ECs, is critical for the inhibition of pro-inflammatory cytokines and leukocyte infiltration in murine viral pneumonia.[33] These results together emphasize the importance of chemerin and its receptor in controlling activated ECs under some inflammatory conditions. NF-κB activation in tumor cells and stromal cell is reported to be important for GM-CSF and IL-6 expression.[27,28] Consistently, we showed that chemerin could inhibit NF-κB activation in tumor cells and tumor-associated ECs via its receptors. However, chemerin had no

effect on the expression of other target genes of NF-κB such as *Il-1β*, *Ccl2* and *Cxcl1/2* in Hepa1-6 tumors. The possible explanation is that other transcriptional factors may be more important for these cytokines, for example, hypoxia inducible factor-1α and signal transducers and activators of transcription 3, were reported to control gene expression of *Il-1β* and *Ccl2* in some chronic inflammatory conditions, including tumors.[34,35] In addition, the inhibitory effect could be cell specific, as IL-1β and CCL2 were found to be primarily expressed by leukocytes and fibroblasts in tumors (unpublished data, Lin *et al.*). It would be interesting to identify the critical target molecule on which chemerin acts to interfere with NF-κB pathway in the future study.

Our study also demonstrated that downregulation of GM-CSF and IL-6 caused by chemerin leads to impaired MDSC induction and consequently decreased tumor-infiltrating MDSCs, which could contribute to HCC inhibition. In contrast to previous study,[24] we found that HCC-inhibitory effect of chemerin is unlikely due to its chemotactic activity toward NK cells. Given that the liver is rich in NK cells,[36] the function, but not the recruitment, of NK cells may be more important in liver diseases. Moreover, we found that HCC-inhibitory effect of chemerin was partly impaired in *Rag1*^{−/−} or CD8+T-cell-depleted mice, suggesting both T-cell-dependent and -independent mechanisms involved. These results together suggest that various mechanisms are involved in the tumor-inhibitory effect of chemerin, which may be dependent on the tumor types. Given that HCC is highly vascularized tumor,[8] T-cell-independent tumor-inhibitory effect of chemerin could be attributed to decreased tumor angiogenesis caused by impaired MDSC accumulation, as chemerin over-expression markedly decreased tumor angiogenesis and the expression of the proangiogenic factors, Bv8 and MMP9, which are primarily secreted by MDSCs.[37] Although chemerin was previously reported to endothelial angiogenesis *in vitro*,[18] our results suggest that the direct inducing effect of chemerin on angiogenesis is minor and overpowered by its strong anti-inflammatory effect *in vivo*.

Enhanced infiltration of TAMs was also found in tumor sites of *Rarres2*^{−/−} mice. This could be due to increased circulating MDSCs, which migrate into tumor sites and differentiate into macrophages under hypoxia.[38] Recent data indicated the importance of MDSCs and macrophages in tumor metastasis,[10,37] which could explain the occurrence of lung metastasis for a low metastatic cell line in *Rarres2*^{−/−} mice. However, it is still possible that chemerin directly modulates the immunosuppressive function of MDSCs and macrophages contributing to tumor suppression, as TAMs are M2-like macrophages and we previously reported that chemerin could inhibit M2 macrophages in a mouse model of acute colitis.[39] In addition, chemerin appeared to cause a shift from Th2 to Th1-type response, as greatly decreased IL-4, but increased IFN-γ expression, were found in the tumor microenvironment, which could antagonize the immunosuppressive function of MDSCs and TAMs.

In summary, our study reveals a novel tumor-inhibitory role of chemerin in HCC by suppressing tumor-associated inflammation, and suggests that reduced endogenous chemerin could contribute to HCC progression. Application of chemerin, therefore, could be a promising therapeutic strategy to potentially inhibit the progression of HCC or other inflammation-driven cancers.

MATERIALS AND METHODS

Human samples
Blood samples and freshly resected tumor and para-tumor tissues from HCC patients were obtained between July 2013 and April 2015, and a cohort of human HCC specimens were randomly collected from 2005 to 2010 in Liver Cancer Institute, Zhongshan Hospital, Fudan University, Shanghai, China. Blood samples from healthy controls were collected from Shanghai Public Health Clinical Center. HCC TMAs were constructed by Shanghai Biochip Co., Ltd (Shanghai, China) as described previously.[40] The researchers who determined chemerin levels were blinded to the clinical information for each patient. All patients and healthy donors provided written informed consent. The study protocol was approved by the Institute Review Board of Fudan University, Zhongshan Hospital.

Mice
Rarres2^{−/−} mice were generated by Cyagen Company (Shanghai, China). Targeting strategy for the disruption of the *Rarres2* gene locus is depicted in Supplementary Figure 1a. Six to 8-week male C57BL/6 WT mice were purchased from Chinese Academy of Sciences (Shanghai, China). B6.129S7-*Rag1*[tm1Mom]/J (*Rag1*^{−/−}) mice were purchased from The Jackson Laboratory (Bar Harbor, ME, USA). All mice were kept and bred in a specific pathogen-free environment. All animal experiments were conducted in accordance with protocols approved by the Animal Care and Use Committee at Fudan University Shanghai Medical College.

Animal tumor model
The number of mice in each group is based on sample size estimate. For orthotopic HCC model, Hepa1-6 cells (5×10^6 cells in 100 μl phosphate-buffered saline) were injected subcutaneously into the left flank region of C57BL/6 mouse. When the tumor reached approximate 1 cm in length, non-necrotic subcutaneous tumor tissue was removed and cut into about 1-mm^3 pieces and implanted into the liver of 6-week-old male *Rarres2*^{−/−} mice or WT littermates. For some experiments, the mice were randomly selected for intravenous injection of the neutralizing antibodies of GM-CSF and IL-6 (each 5 mg/kg) (both from eBioscience, San Diego, CA, USA) every 2 days from 2 weeks following the liver implantation until the mice were killed. The researchers who measured tumor size were blinded to treatment.

Histological analysis and IHC
For IHC, briefly, after antigen retrieval, mouse liver tumor sections were incubated with the antibodies against Gr-1 (RB-8C5; 1:200, MCA2387, AbDserotech, Oxford, UK), F4/80 (BM8; 1:200, MCA497, AbDserotech), CD31 (M-20) (1:200, sc-1506, Santa Cruz Biotechnology, Santa Cruz, CA, USA), or sections from human HCC TMA were incubated with the antibodies against human chemerin (1:200, AF2324, R&D Systems, Inc., Minneapolis, MN, USA), CD56 (1:200, ab191105, Abcam, Cambridge, MA, USA); CD11b (M1/70) (1:500, ab64347, Abcam) overnight at 4 °C, followed by the secondary antibody incubation ABC kits (Vector Lab, Burlingame, CA, USA). For evaluation of IHC, the staining-positive cells were counted blinded in 10 high-power fields at 400X or 200X. According to previous studies,[40–42] chemerin density was measured by Image-Pro Plus v6.2 software (Media Cybernetics Inc., Sliver Spring, MD, USA), and CD31-positive vessels with a clearly defined lumen or well-defined linear vessel shapes were considered to assess microvessel density.

Flow cytometry
The following fluorochrome-labeled anti-mouse Abs were used: CD45 (30-F11), CD11b (M1/70), Gr-1 (RB6-8C5), F4/80 (BM8), CD4 (GK1.5), CD8 (APA5), IFN-γ (AN-18), NK1.1 (PK136), CD3 (17A2), CD31 (390), PDGFRα (53-6.7), EpCAM (1B7; all from eBioscience), CCRL2 (MAB5519, R&D Systems, Inc.) and isotype antibodies (eBioscience). ChemR23 was labeled by goat-anti-mChemR23 (sc-32652, Santa Cruz Biotechnology) followed by flurochrome-labeled anti-goats secondary antibody. Samples were acquired by Cyan instrument (Beckman Coulter, Miami, FL, USA) and analyzed by FlowJo software (Treestar, Inc., San Carlos, CA, USA). For some experiments, single-cell suspensions of tumor tissues were further separated by Moflow (Beckman Coulter) into individual cell populations: tumor cells (EpCAM$^+$CD45$^-$); leukocytes (CD45$^+$CD31$^-$); fibroblasts (CD45$^-$PDGFRα$^+$CD31$^-$) and ECs (CD31$^+$CD45$^-$EpCAM$^-$).

Statistical analysis
The comparisons between two groups were performed by two-tailed Student's *t*-tests. Multiple-group comparisons were performed by analysis of variance followed by a Bonferroni correction to compare each group. Survival was determined by Kaplan–Meier method and survival curves between different groups were calculated by log-rank test. The preoperative clinical data, intraoperative and pathological findings,

postoperative mortality, overall survival and time to recurrence were compared between patients with high and low expression of chemerin. The χ^2 test or Fisher's exact test was used for qualitative variables comparison. All statistical tests were justified as appropriate and all data meet the assumptions of the tests. The variance is similar between the groups that were being statistically compared. The sample size was estimated by pre-determined tables for certain values to ensure the adequate power to detect a pre-specified effect size. The statistical analysis was performed with SPSS 19.0 for Windows (SPSS Inc., Chicago, IL, USA).

Additional Materials and Methods can be found in the Supplementary Information.

CONFLICT OF INTEREST

The authors declare no conflict of interest.

REFERENCES

1 Makarova-Rusher OV, Medina-Echeverz J, Duffy AG, Greten TF. The yin and yang of evasion and immune activation in HCC. *J Hepatol* 2015; **62**: 1420–1429.

2 Gabrilovich DI, Nagaraj S. Myeloid-derived suppressor cells as regulators of the immune system. *Nat Rev Immunol* 2009; **9**: 162–174.

3 Ostrand-Rosenberg S, Sinha P. Myeloid-derived suppressor cells: linking inflammation and cancer. *J Immunol* 2009; **182**: 4499–4506.

4 Hoechst B, Ormandy LA, Ballmaier M, Lehner F, Kruger C, Manns MP et al. A new population of myeloid-derived suppressor cells in hepatocellular carcinoma patients induces CD4(+)CD25(+)Foxp3(+) T cells. *Gastroenterology* 2008; **135**: 234–243.

5 Arihara F, Mizukoshi E, Kitahara M, Takata Y, Arai K, Yamashita T et al. Increase in CD14+HLA-DR -/low myeloid-derived suppressor cells in hepatocellular carcinoma patients and its impact on prognosis. *Cancer Immunol Immunother* 2013; **62**: 1421–1430.

6 Hoechst B, Voigtlaender T, Ormandy L, Gamrekelashvili J, Zhao F, Wedemeyer H et al. Myeloid derived suppressor cells inhibit natural killer cells in patients with hepatocellular carcinoma via the NKp30 receptor. *Hepatology* 2009; **50**: 799–807.

7 Condamine T, Gabrilovich DI. Molecular mechanisms regulating myeloid-derived suppressor cell differentiation and function. *Trends Immunol* 2011; **32**: 19–25.

8 Zhu AX, Duda DG, Sahani DV, Jain RK. HCC and angiogenesis: possible targets and future directions. *Nat Rev Clin Oncol* 2011; **8**: 292–301.

9 Wong VW, Yu J, Cheng AS, Wong GL, Chan HY, Chu ES et al. High serum interleukin-6 level predicts future hepatocellular carcinoma development in patients with chronic hepatitis B. *Int J Cancer* 2009; **124**: 2766–2770.

10 Su S, Liu Q, Chen J, Chen F, He C, Huang D et al. A positive feedback loop between mesenchymal-like cancer cells and macrophages is essential to breast cancer metastasis. *Cancer Cell* 2014; **25**: 605–620.

11 Dolcetti L, Peranzoni E, Ugel S, Marigo I, Fernandez Gomez A, Mesa C et al. Hierarchy of immunosuppressive strength among myeloid-derived suppressor cell subsets is determined by GM-CSF. *Eur J Immunol* 2010; **40**: 22–35.

12 Chen MF, Kuan FC, Yen TC, Lu MS, Lin PY, Chung YH et al. IL-6-stimulated CD11b+ CD14+ HLA-DR- myeloid-derived suppressor cells, are associated with progression and poor prognosis in squamous cell carcinoma of the esophagus. *Oncotarget* 2014; **5**: 8716–8728.

13 Wittamer V, Franssen JD, Vulcano M, Mirjolet JF, Le Poul E, Migeotte I et al. Specific recruitment of antigen-presenting cells by chemerin, a novel processed ligand from human inflammatory fluids. *J Exp Med* 2003; **198**: 977–985.

14 Goralski KB, McCarthy TC, Hanniman EA, Zabel BA, Butcher EC, Parlee SD et al. Chemerin, a novel adipokine that regulates adipogenesis and adipocyte metabolism. *J Biol Chem* 2007; **282**: 28175–28188.

15 Parolini S, Santoro A, Marcenaro E, Luini W, Massardi L, Facchetti F et al. The role of chemerin in the colocalization of NK and dendritic cell subsets into inflamed tissues. *Blood* 2007; **109**: 3625–3632.

16 Albanesi C, Scarponi C, Pallotta S, Daniele R, Bosisio D, Madonna S et al. Chemerin expression marks early psoriatic skin lesions and correlates with plasmacytoid dendritic cell recruitment. *J Exp Med* 2009; **206**: 249–258.

17 Monnier J, Lewen S, O'Hara E, Huang K, Tu H, Butcher EC et al. Expression, regulation, and function of atypical chemerin receptor CCRL2 on endothelial cells. *J Immunol* 2012; **189**: 956–967.

18 Kaur J, Adya R, Tan BK, Chen J, Randeva HS. Identification of chemerin receptor (ChemR23) in human endothelial cells: chemerin-induced endothelial angiogenesis. *Biochem Biophys Res Commun* 2010; **391**: 1762–1768.

19 Zabel BA, Nakae S, Zuniga L, Kim JY, Ohyama T, Alt C et al. Mast cell-expressed orphan receptor CCRL2 binds chemerin and is required for optimal induction of IgE-mediated passive cutaneous anaphylaxis. *J Exp Med* 2008; **205**: 2207–2220.

20 Bondue B, Wittamer V, Parmentier M. Chemerin and its receptors in leukocyte trafficking, inflammation and metabolism. *Cytokine Growth Factor Rev* 2011; **22**: 331–338.

21 Zhao L, Yang W, Yang X, Lin Y, Lv J, Dou X et al. Chemerin suppresses murine allergic asthma by inhibiting CCL2 production and subsequent airway recruitment of inflammatory dendritic cells. *Allergy* 2014; **69**: 763–774.

22 Imai K, Takai K, Hanai T, Shiraki M, Suzuki Y, Hayashi H et al. Impact of serum chemerin levels on liver functional reserves and platelet counts in patients with hepatocellular carcinoma. *Int J Mol Sci* 2014; **15**: 11294–11306.

23 Lin W, Chen YL, Jiang L, Chen JK. Reduced expression of chemerin is associated with a poor prognosis and a lowed infiltration of both dendritic cells and natural killer cells in human hepatocellular carcinoma. *Clin Lab* 2011; **57**: 879–885.

24 Pachynski RK, Zabel BA, Kohrt HE, Tejeda NM, Monnier J, Swanson CD et al. The chemoattractant chemerin suppresses melanoma by recruiting natural killer cell antitumor defenses. *J Exp Med* 2012; **209**: 1427–1435.

25 Youn JI, Nagaraj S, Collazo M, Gabrilovich DI. Subsets of myeloid-derived suppressor cells in tumor-bearing mice. *J Immunol* 2008; **181**: 5791–5802.

26 Murdoch C, Muthana M, Coffelt SB, Lewis CE. The role of myeloid cells in the promotion of tumour angiogenesis. *Nat Rev Cancer* 2008; **8**: 618–631.

27 He G, Karin M. NF-kappaB and STAT3 - key players in liver inflammation and cancer. *Cell Res* 2011; **21**: 159–168.

28 Park BK, Zhang H, Zeng Q, Dai J, Keller ET, Giordano T et al. NF-kappaB in breast cancer cells promotes osteolytic bone metastasis by inducing osteoclastogenesis via GM-CSF. *Nat Med* 2007; **13**: 62–69.

29 Barnea G, Strapps W, Herrada G, Berman Y, Ong J, Kloss B et al. The genetic design of signaling cascades to record receptor activation. *Proc Natl Acad Sci USA* 2008; **105**: 64–69.

30 Wanninger J, Bauer S, Eisinger K, Weiss TS, Walter R, Hellerbrand C et al. Adiponectin upregulates hepatocyte CMKLR1 which is reduced in human fatty liver. *Mol Cell Endocrinol* 2012; **349**: 248–254.

31 Fisher DT, Appenheimer MM, Evans SS. The two faces of IL-6 in the tumor microenvironment. *Semin Immunol* 2014; **26**: 38–47.

32 Teijaro JR, Walsh KB, Cahalan S, Fremgen DM, Roberts E, Scott F et al. Endothelial cells are central orchestrators of cytokine amplification during influenza virus infection. *Cell* 2011; **146**: 980–991.

33 Bondue B, Vosters O, de Nadai P, Glineur S, De Henau O, Luangsay S et al. ChemR23 dampens lung inflammation and enhances anti-viral immunity in a mouse model of acute viral pneumonia. *PLoS Pathog* 2011; **7**: e1002358.

34 Yang S, Wang B, Humphries F, Hogan AE, O'Shea D, Moynagh PN. The E3 ubiquitin ligase Pellino3 protects against obesity-induced inflammation and insulin resistance. *Immunity* 2014; **41**: 973–987.

35 Tsuyada A, Chow A, Wu J, Somlo G, Chu P, Loera S et al. CCL2 mediates cross-talk between cancer cells and stromal fibroblasts that regulates breast cancer stem cells. *Cancer Res* 2012; **72**: 2768–2779.

36 Tian Z, Chen Y, Gao B. Natural killer cells in liver disease. *Hepatology* 2013; **57**: 1654–1662.

37 Condamine T, Ramachandran I, Youn JI, Gabrilovich DI. Regulation of tumor metastasis by myeloid-derived suppressor cells. *Annu Rev Med* 2015; **66**: 97–110.

38 Corzo CA, Condamine T, Lu L, Cotter MJ, Youn JI, Cheng P et al. HIF-1alpha regulates function and differentiation of myeloid-derived suppressor cells in the tumor microenvironment. *J Exp Med* 2010; **207**: 2439–2453.

39 Lin Y, Yang X, Yue W, Xu X, Li B, Zou L et al. Chemerin aggravates DSS-induced colitis by suppressing M2 macrophage polarization. *Cell Mol Immunol* 2014; **11**: 355–366.

40 Gao Q, Qiu SJ, Fan J, Zhou J, Wang XY, Xiao YS et al. Intratumoral balance of regulatory and cytotoxic T cells is associated with prognosis of hepatocellular carcinoma after resection. *J Clin Oncol* 2007; **25**: 2586–2593.

41 Zhang JP, Yan J, Xu J, Pang XH, Chen MS, Li L et al. Increased intratumoral IL-17-producing cells correlate with poor survival in hepatocellular carcinoma patients. *J Hepatol* 2009; **50**: 980–989.

42 Zhu XD, Zhang JB, Zhuang PY, Zhu HG, Zhang W, Xiong YQ et al. High expression of macrophage colony-stimulating factor in peritumoral liver tissue is associated with poor survival after curative resection of hepatocellular carcinoma. *J Clin Oncol* 2008; **26**: 2707–2716.

Supplementary Information accompanies this paper on the Oncogene website (http://www.nature.com/onc)